Response to editor's comments

We first outline the major changes made to the manuscript in the light of the editor's comments, and then respond to individual comments. Our responses are in italics, and revised text is given in normal script in blue. We have updated the reference list in the revised manuscript to include the new references involved.

Major changes to the manuscript

1. Expansion of the fossil pollen dataset

We originally based our analyses on the records in the ACER database. In our discussion, we acknowledged that several new records had become available since the ACER database was published. The editor kindly pointed out some additional papers related to Lake Bergsee and suggested we refer to this. On investigation, we realised that there are a very large number of new records and decided to create an updated version of the ACER database: ACER2. Unfortunately, there was no response to our request for the pollen from Lake Bergsee.

The use of a much-expanded set greatly fills in the spatial gaps of original ACER database, especially in Siberia and China, which makes our conclusions more strongly supported by the evidence: the largest warming still occurred in northern extratropics, especially Eurasia, while western North America and the southern extratropics were still characterised by cooling; the change in winter temperature was still significantly larger than the change in summer temperature in the northern extratropics, indicating that the D-O warming events were characterised by reduced seasonality, but there was still no significant difference between the summer and winter temperature changes in the southern extratropics.

The spatial distribution of records in original ACER database:

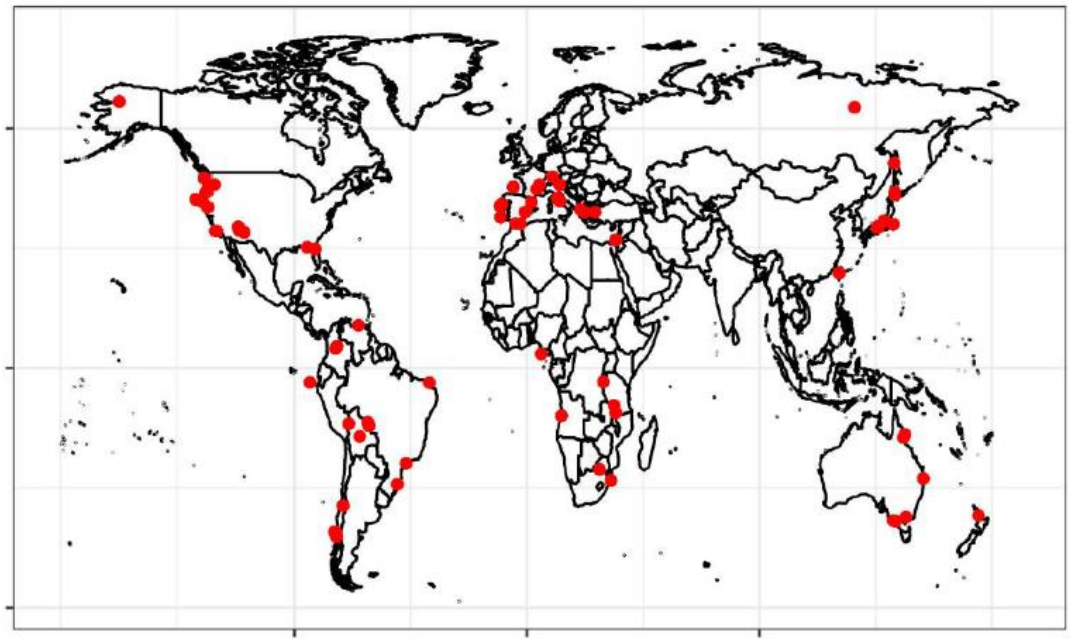

The spatial distribution of records in revised manuscript (ACER + ACER2):

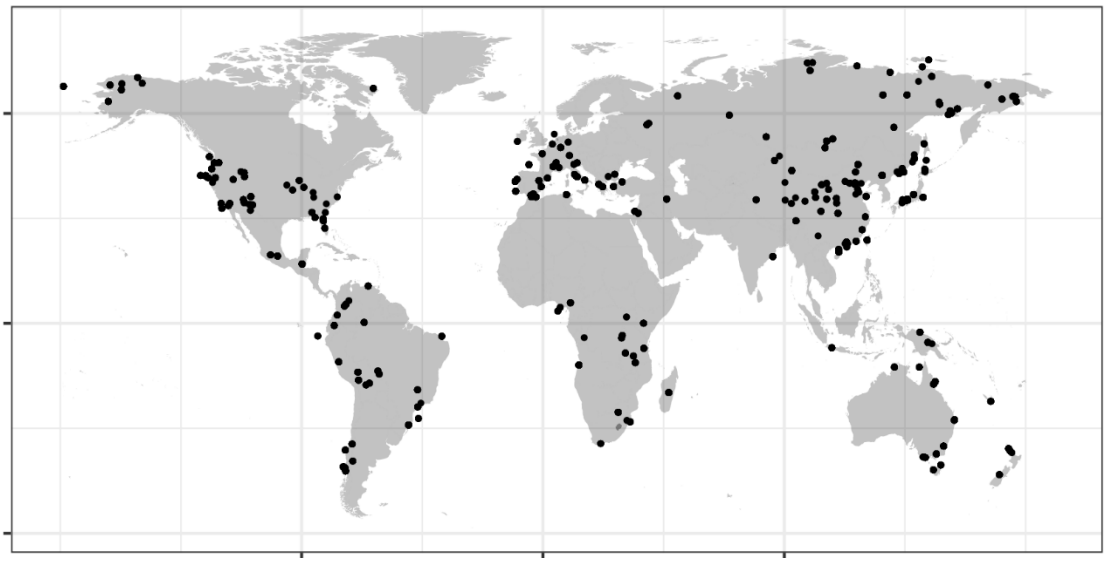

In the light of these major changes to the manuscript, we have modified our Methods section as follows (see final paragraph of section 2.1 in revised manuscript):

The Abrupt Climate Changes and Environmental Responses (ACER) database (Sánchez-Goñi et al., 2017) was originally created to provide a source of pollen and charcoal data for Marine Isotope Stage 3 (MIS 3), which includes 93 records with sufficient resolution and dating control to detect sub-millennial scale variability. Much more records covering MIS 3 have become available since the compilation of the ACER database, such as the synthetic pollen databases available for Siberia (Cao et al., 2019, 2020) and China (Zhou et al., 2023) and the global Legacy 2 dataset (Li et al., 2025), which can substantially cover the spatial gaps in the original ACER database. We obtained these data from public sources or directly from the authors and used them to create an update: ACER2 (Harrison et al., 2025b), which contains 233 additional records covering some part or all of MIS 3 (note that the original ACER records are not included in ACER2 due to licensing issue). The two datasets are combined in our analyses to serve as the fossil pollen dataset (Supplementary Materials, section 3) to reconstruct the past climates. We focus on the 279 records (253 terrestrial records and 26 marine records) between 50 and 30 ka (Figure 1b; Table 1). The fossil pollen data were taxonomically harmonised to be consistent with the SMPDSv3.

We have updated Figure 1 and Table 1 to include the ACER2 sites and we have also updated Section 3 in the Supplementary to include the appropriate references for these sites. We have also updated the Acknowledgements to thank the authors who provided data directly for the ACER2 compilation as follows:

ML acknowledges support from Imperial College through the Lee Family Scholarship. ICP acknowledges support from the ERC under the European Union Horizon 2020 research and innovation programme (grant agreement no.: 787203 REALM). SPH acknowledges fruitful discussions with colleagues from the D-O community working group. We would like to acknowledge our colleagues who provided original pollen data for inclusion in the ACER2 data set: Jon Camuera, Penelope González-Sampériz, Gonzalo Jiménez-Moreno, Xinghi Liu, Rewi Newnham, Jian Ni, Roberta Pini, Cassie Rowe, Frank Sirocco and María Del Socorro Lozano-García.

We have removed the final sentence of the discussion (shown below), since this is no longer relevant, and the references cited therein are included in our new Table 1.

~~Several new high-resolution records covering MIS3 have become available since the compilation of the ACER database (e.g. Bird et al., 2024; Wei et al., 2021; Camuera et al., 2022; Pini et al., 2022; Rowe et al., 2024; Shichi et al., 2023; Zorzi et al., 2022) and including these newer records could help to improve the reliability of the global reconstructions presented here.~~

2. The CO_2 correction on the plant-available moisture

We have added the following text in the Methods to give more information (see section 2.2 in revised manuscript):

However, the low CO_2 at glacial period could lead to potential bias between reconstructed and actual plant-available moisture. Atmospheric CO_2 concentration has a direct impact on plant physiological processes, by modulating water-use efficiency (WUE), that is the ratio of carbon uptake to water loss through the stomata (Hatfield and Dold, 2019). The low CO_2 during the glacial period led to reduced water use efficiency (Farquhar, 1997; Gerhart and Ward, 2010; Prentice and Harrison, 2009). Statistical reconstructions cannot take this into account since they are based on modern relationships between pollen assemblages and climate under recent CO_2 levels (Bartlein et al., 2011; Chevalier et al., 2020). The actual conditions under low CO_2 should be wetter than the vegetation-based reconstructions of moisture variables (Prentice et al., 2017, 2022a). Prentice et al. (2022a) provides a way of correction as follows:

$$e(MTGR_1, MI_1, c_{a1}) = e(MTGR_0, MI_0, c_{a0}) \quad (1)$$

where e is the ratio of water loss to CO_2 uptake, a function of the mean temperature of the growing season (MTGR), moisture index (MI) and atmospheric CO_2 concentration (c_a). For MTGR and c_a, the subscript "1" denotes the past value, and the subscript "0" denotes the modern value. MI_0 is the reconstructed uncorrected past value, MI_1 is the "true" past value (to be estimated). The equation means that the "true" MI under past atmospheric conditions should produce the same e with the reconstructed uncorrected MI under modern atmospheric conditions, i.e. those pertaining to the modern pollen calibration dataset.

We transferred our reconstructed past α_{plant} back to the uncorrected moisture index MI_0, and applied the CO_2 correction to obtain the actual moisture index MI_1, then transferred it to actual plant-available moisture $\alpha_{plant,corrected}$ (Figure 2; Figure S2-1 & S2-2). Past and modern values of CO_2 concentrations were taken from Bereiter et al. (2015), following Prentice et al. (2022a). Past MTGR values were inferred by sinusoidal interpolation of reconstructed MTCO and MTWA, assuming that the growing season corresponds to the period with temperatures > 0˚C. Modern MTGR values were obtained using a geographically-weighted regression (GWR) of climatological values (1961-1990) from the Climatic Research Unit Time-Series version 4.04 (CRU TS4.04; Harris et al., 2020) dataset averaged over the period 1961–1990, in order to correct for elevation differences between the CRU grid cells and the fossil pollen sites. The elevations of marine sites were set to 0 when applying GWR.

We found that the original correction algorithm of Prentice et al. (2022a) (implemented in previous round of revision) has some parameters too sensitive to the temperature, producing an unrealistically large countervailing effect (drier rather than wetter) and also influencing the significance of the ratio of $\Delta\alpha_{plant,corrected}$ to $\Delta MTWA$. In this version, we applied a modification to the correction algorithm:

The CO_2 correction was implemented through the package COdos 0.0.2 (Prentice et al., 2022b) with one modification, as follows. We found when applying the correction in cases where the temperature reduction from modern was large (> 5˚C) that the use of different temperature values to calculate the stomatal sensitivity term (ξ) and the compensation point (Γ^*) in the correction algorithm sometimes produced an unrealistically large countervailing effect due to the temperature difference alone. To avoid this problem, we calculated these physiological quantities (ξ and Γ^*) using the mean of $MTGR_1$ and $MTGR_0$.

The spatial patterns don't change much compared to previous round of revision. However, the ratio of $\Delta\alpha_{plant,corrected}$ to $\Delta MTWA$ is no longer significantly positive globally. We have updated related figures and tables. We have also added some text in the Discussions to compare the corrected and uncorrected plant-available moisture (see the end of section 4.1 in revised manuscript):

We have applied a correction for low CO_2 values during the glacial period to plant-available moisture. The actual values ($\alpha_{plant,corrected}$) are generally higher than the vegetation-based reconstructed values (α_{plant}) (Figure S2-1). However, the correction does not have a significant impact on the spatial patterns during D-O events (Figure S2-2; Figure S7-3).

Figure S2-1: Comparison of plant-available moisture values before and after CO_2 correction. The black line is the 1:1 line. The colours indicate the past atmospheric CO_2 concentrations.

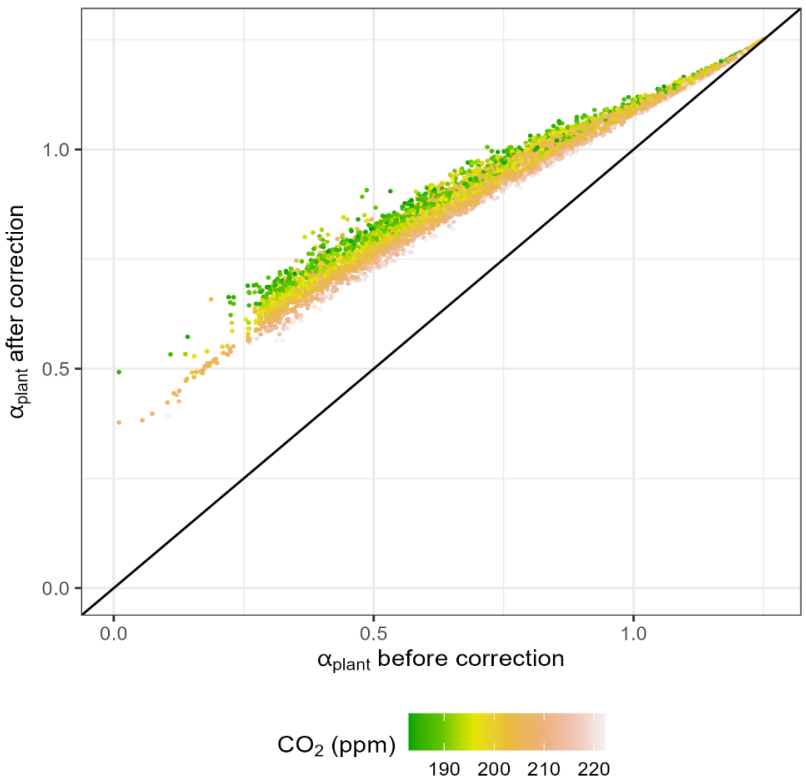

Figure 5: Map showing the median change of site-based reconstructions for Dansgaard-Oeschger (D-O) events 5 to 12. The panels from top to bottom show the changes in mean temperature of the coldest month (ΔMTCO), mean temperature of the warmest month (ΔMTWA) and CO_2-corrected plant-available moisture ($\Delta\alpha_{plant,corrected}$).

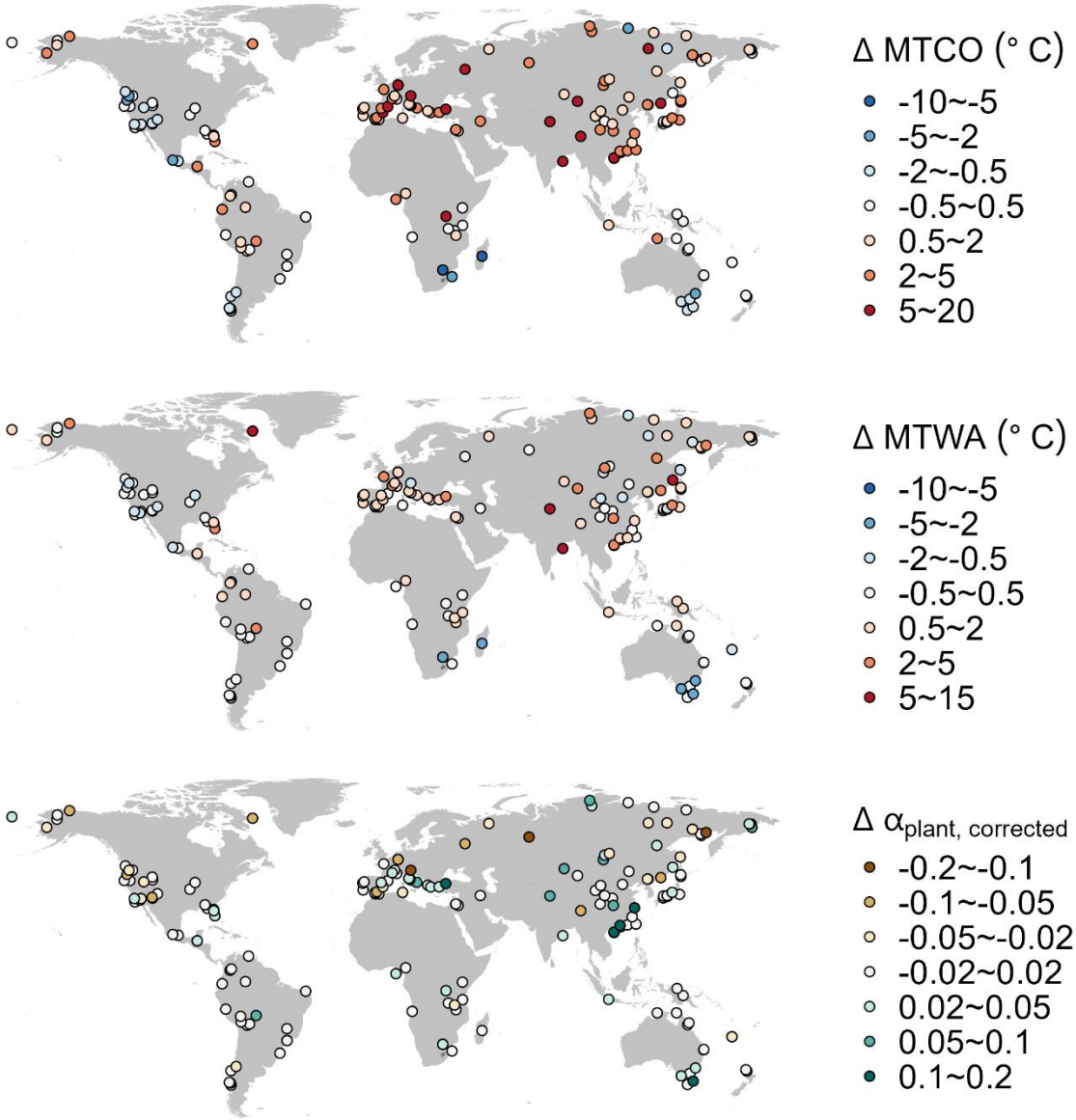

Figure S2-2: Map showing the median change of uncorrected plant-available moisture for Dansgaard-Oeschger (D-O) events 5 to 12. The upper panel is made using all samples. The lower panel is made only using those with |reconstructed change| ≥ 2 |error of change|.

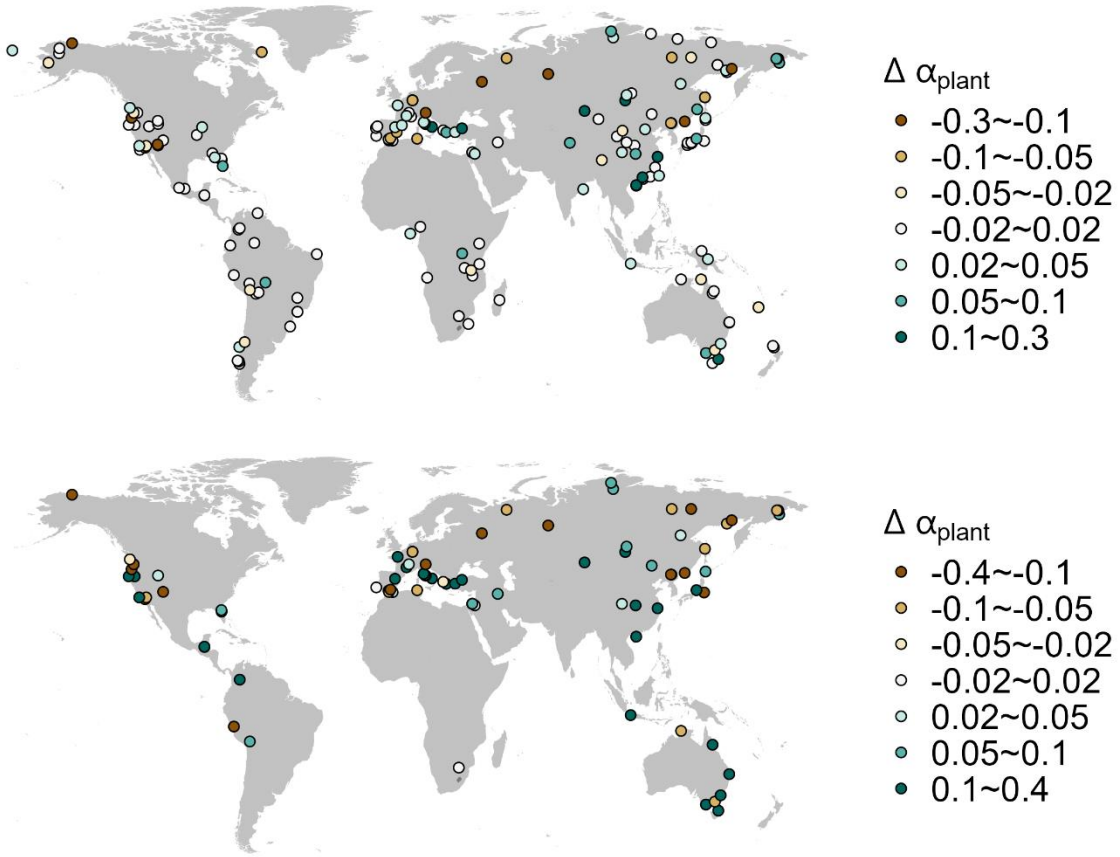

3. Comparison of the reconstructions with models

We have moved the original Figure S9.1 & 9.2 into the main text as Figure 7 (spatial pattern of median change) & Figure 8 (relationship between ΔMTCO and ΔMTWA). We have also moved the original supplementary Table 3 into the main text as Table 5 (maximum likelihood estimation of the ratio of ΔMTCO vs ΔMTWA). We only keep the ice-free land part in Figure 7 to avoid confusion of what is used in Figure 8 and Table 5. We have also modified the discussions as follows (see section 4.3 in revised manuscript):

The reconstructions in this paper can be used as targets for model evaluation, specifically the two transient D-O experiments planned for the next phase of the Palaeoclimate Modelling Intercomparison (see Malmierca-Vallet et al., 2023 for the experimental protocol). The first of these experiments is a baseline simulation starting at 34 ka, a time with low obliquity, moderate MIS3 greenhouse gas values, and an intermediate ice sheet configuration, which appears to be most conducive to generating D-O like behaviour in climate models. The second experiment involves the addition of freshwater, to examine whether this is necessary to precondition a state conducive to generating D-O events. The anti-phasing in reconstructed temperature changes between the northern and southern hemispheres is a general feature of

climate model experiments. Most models show larger warming in winter than in summer in the northern hemisphere (e.g. Flückiger et al., 2008; Izumi et al., 2023; Van Meerbeeck et al., 2011), which is also consistent with our reconstructions. However, the cooling in western North America during D-O warming events in our reconstructions is not a feature of all climate model simulations.

Models generally show an intensification of the northern hemisphere monsoons during D-O events (e.g. Izumi et al., 2023; Menviel et al., 2020), but there is less consistency about changes in plant-available moisture in the extratropics. Our reconstructions show an increase in $\alpha_{plant,corrected}$ in southeastern China and Japan (Figure 5). Although $\alpha_{plant,corrected}$ is not a direct reflection of summer precipitation, these changes are consistent with enhanced northern hemisphere monsoons during D-O warming events, as shown by speleothem records from the Caribbean (Warken et al., 2019) and speleothem and pollen records from Asia (Fohlmeister et al., 2023; Wang et al., 2001; Zorzi et al., 2022). However, there are more spatial variability and mixed signals.

The LOVECLIM model was used as a reference to adjust the age scale in the reconstructions using MAT, but this does not preclude comparison of the seasonal temperatures. Here we approximate the winter-season temperature as MTCO and summer-season temperature as MTWA, since monthly temperatures are not available (only seasonal temperatures are available) in LOVECLIM. The general spatial pattern of simulated changes in MTCO and MTWA (Figure 7) is consistent with the reconstructions, with largest warming in Eurasia, and cooling in the southern extratropics. The simulated changes are strong during D-O 8 but weak during D-O 9 (Figures 9-1 & 9-2), again as shown by the reconstructions. However, there are important differences. For example, simulated changes generally have smaller amplitude than shown by the reconstructions, and the cooling over western North America is generally only in winter, while the reconstructions show cooling over this region in both seasons. The relationship between ΔMTCO and ΔMTWA is also different (Figure 8; Table 5): the simulated ΔMTCO is shown to be significantly larger than ΔMTWA in the northern extratropics, but significantly smaller than ΔMTWA in the southern extratropics, a contrast that is not so marked in the reconstructions. This comparison illustrates the usefulness of the reconstructions for model evaluation and to investigate the mechanisms that may not be adequately captured by current models.

4. The variability between individual D-O events

We have added a paragraph in the introduction as follows (see second paragraph of section 1 in revised manuscript):

Although D-O events are found throughout the last glacial period, the largest number and the most regular patterning occurred during Marine Isotope Stage 3 (MIS 3; 57 to 29 ka) when there were 11 separate events (D-O 15 to D-O 5), while earlier stage such as MIS 4 (71 to 57 ka) only had 3 separate events (D-O 18 to 16). The typical duration of a cycle as manifested in Greenland is *ca.* 1500 years and is characterised by an initial short slow warming, followed by an abrupt large warming in matter of decades, followed by a long slow cooling over centuries to millennia, with a terminal phase of fast cooling (e.g. D-O 8, D-O 12). However, there are also cycles in which the warming and cooling phases took roughly the same time

(e.g. D-O 5, D-O 6, D-O 9). The magnitude of changes also differ, with both strong events (e.g. D-O 8, D-O 12) and weak events (e.g. D-O 9).

We have also added some text (see fourth and fifth paragraph of section 3 in revised manuscript) and a new figure comparing a weak event and a strong event.

The spatial patterns of ΔMTCO and ΔMTWA are generally consistent across multiple D-O events (Figure 5), most noticeably that the largest warming occurs in Eurasia, while western North America and the southern extratropics are characterised by cooling. These patterns are also shown if only reconstructions where the change is twice the error of change are considered (Figure S6), proving that the spatial patterns are robust to the choice of threshold. Nevertheless, both the magnitude of the changes and the spatial patterns vary between the D-O events (Figures S7-1 & S7-2). Strong events such as D-O 8 show more apparent changes (whether warming or cooling), as well as a strong antiphasing between northern and southern extratropical changes; while weak events such as D-O 9 show less apparent changes with almost no north-south antiphasing (Figure 6).

The changes in plant-available moisture are less spatially coherent that the changes in temperature (Figure 5). There is an increase in $\alpha_{plant,corrected}$ in some regions characterised by warming, for example, southeastern China and Japan; but there are mixed signals of drying and wetting in other regions characterised by warming, such as southern Europe. Furthermore, regions characterised by cooling, such as western North America and southern extratropics, can also show both drying and wetting. Changes in $\Delta\alpha_{plant,corrected}$ also show more variability between D-O events than temperature (Figure S7-4).

The added figure 6 is as below:

Figure 6: Map showing the change in mean temperature of the coldest month (ΔMTCO) and the change in mean temperature of the warmest month (ΔMTWA) for D-O 9 (a weak event) and D-O 8 (a strong event). The upper panel shows ΔMTCO, while the lower panel shows ΔMTWA.

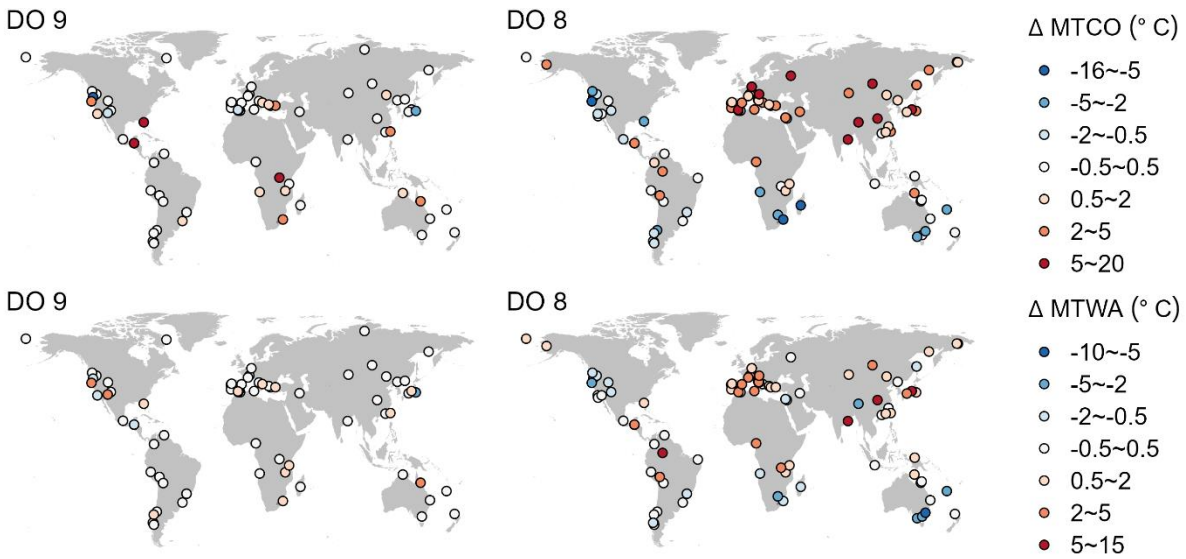

5. The atmospheric and oceanic mechanisms that could explain the obtained results, particularly the observed winter/summer decoupling

The anti-phasing between northern and southern extratropics and the reduction in seasonality in the northern extratropics, are consistent with a number of different proposed mechanisms. The reconstructions of themselves do not address potential causes or mechanisms, but we have expanded the text to indicate the degree to which the patterns shown are consistent with model experiments that address the potential mechanisms underlying these changes. Please see section 4.3 in revised manuscript.

6. Comparison with other regional studies, particularly Zumarque et al. (2025)

We have added the following text (see section 4.1 in revised manuscript):

We have presented a first attempt to map the spatial patterns of quantitative changes in seasonal temperatures and plant-available moisture during D-O events globally, using a consistent methodology. These analyses show that there is an anti-phasing between changes in the northern extratropics and the southern extratropics, with warming in the north and cooling in the south. The largest and most consistent warming during D-O events occurs in Eurasia. There is a significant difference between winter warming and summer warming in the northern extratropics, resulting in an overall reduction in seasonality. Site-based reconstructions from the Eifel region in central Europe, based on branched glycerol dialkyl glycerol tetraethers, indicate minimal temperature changes during summer (Zander et al., 2024) and thus support the idea that the D-O changes were driven by large changes in winter temperature. Zumaque et al., (2025) provide seasonal temperature and precipitation reconstructions for 12 of the sites from southern Europe (which are included in our fossil pollen records) but using the modern analogue technique as the reconstruction method and the Eurasian Modern Pollen Database version 2 (Davis et al., 2020) (EMPDv2; also included in our SMPDSv3) as the modern training dataset. They show relatively stable summer temperatures but large change in MTCO through the MIS3 D-O events, consistent with our reconstructions (using a regression-based reconstruction method and a global modern training dataset) of a reduction in seasonality during warming events in the northern extratropics. We found no significant difference in the magnitude of seasonal warming in the southern extratropics. Since only quantitative reconstructions of MAT (rather than MTCO and MTWA) are available from the southern extratropics (e.g. Fletcher and Thomas, 2010; Newnham et al., 2017), there is no independent confirmation of this result.

Qualitative interpretation of palaeo-records suggest that some many regions were characterised by both warming and wetting, such as western Europe (Fletcher et al., 2010; Sánchez-Goñi et al., 2008), eastern Europe (Fleitmann et al., 2009; Stockhecke et al., 2016), central Siberia (Grygar et al., 2006), and the Great Basin USA (Denniston et al., 2007; Jiménez-Moreno et al., 2010). Previous studies have also indicated drier conditions during D-O events, particularly in parts of the USA such as the Pacific Northwest (Grigg and Whitlock, 2002) and Florida (Grimm et al., 2006; Jiménez-Moreno et al., 2010). Our reconstructions show more mixed signals and that there is no globally consistent relationship between changes in MTWA and moisture, either in regions characterised by warming or by cooling (Figure 4; Figure 5). We have applied a correction for low CO_2 values during the glacial period to plant-available moisture. The actual values ($\alpha_{plant,corrected}$) are generally higher than the vegetation-based reconstructed values (α_{plant}) (Figure S2-1). However, the correction does

not have a significant impact on the spatial patterns during D-O events (Figure S2-2; Figure S7-3).

Other points

7. Line 44. Please provide more detail about D/O cycles, including how many occurred during MIS 4 and 3, their typical duration, and specific features of the key D/O events. It would also be helpful to briefly summarize what is currently known about their variability.

We have expanded the description of the D-O cycles in the introduction, and what is known about their expression from different kinds of records as follows:

Although D-O events are found throughout the last glacial period, the largest number and the most regular patterning occurred during Marine Isotope Stage 3 (MIS 3; 57 to 29 ka) when there were 11 separate events (D-O 15 to D-O 5), while earlier stage such as MIS 4 (71 to 57 ka) only had 3 separate events (D-O 18 to 16). The typical duration of a cycle as manifested in Greenland is *ca.* 1500 years and is characterised by an initial short slow warming, followed by an abrupt large warming in matter of decades, followed by a long slow cooling over centuries to millennia, with a terminal phase of fast cooling (e.g. D-O 8, D-O 12). However, there are also cycles in which the warming and cooling phases took roughly the same time (e.g. D-O 5, D-O 6, D-O 9). The magnitude of changes also differ, with both strong events (e.g. D-O 8, D-O 12) and weak events (e.g. D-O 9).

The D-O signals are not just in Greenland – they are registered globally (Adolphi et al., 2018; Corrick et al., 2020; Harrison and Sanchez-Goñi, 2010; Sánchez-Goñi et al., 2017; Voelker, 2002) and are reflected in changes in both temperature and precipitation. Both oceanic and ice-core records indicate that temperature changes are out-of-phase between the northern and southern hemispheres, and the southern hemisphere response both in terms of warming and cooling phases is generally less abrupt (Dima et al., 2018; Vettoretti and Peltier, 2015). There is a comparative lack of information from the continents about the manifestation of D-O events. Shifts in vegetation types between GI and GS states have been interpreted as primarily a temperature signal in the extratropics and a moisture signal in the tropics (Harrison and Sanchez-Goñi, 2010). Speleothem records provide a good time-control on the synchroneity of climate changes globally with the D-O events registered in Greenland (Adolphi et al., 2018; Corrick et al., 2020), but the driver of this signal can either be temperature or precipitation depending on the region. There are quantitative climate reconstructions based on terrestrial pollen records from La Grande Pile (Guiot et al., 1993), Lago Grande di Monticchio (Huntley et al., 1999), Padul (Camuera et al., 2022), El Cañizar de Villarquemado (Camuera et al., 2022; Wei et al., 2021) and Lake Ohrid (Sinopoli et al., 2019), marine cores in the western Mediterranean and offshore from Portugal (Sánchez-Goñi et al., 2002), diatom assemblages at Les Echets, France (Ampel et al., 2010), chironomids from Lake Bergsee in central Europe (Lapellegerie et al., 2024), bacterial membrane lipid records from the Eifel region (Zander et al., 2024), isotopic measurements of earthworm calcite from the Rhine Valley (Prud'homme et al., 2022) and clumped isotope measurements on snails in Hungary (Újvári et al., 2021). Aside from the lack of comparable quantitative estimates from outside Europe, differences in the methodology employed and in the specific climate variables reconstructed in each of these studies limits their usefulness for model

evaluation. In particular, given that there is still uncertainty as to whether the D-O cycles are characterised by changes in seasonality such that warming events are primarily driven by changes in winter (Flückiger et al., 2008; Zander et al., 2024; Zumaque et al., 2025), in the regional strength of the warming (Harrison and Sanchez-Goñi, 2010) and how warming relates to changes in moisture (Wei et al., 2021), there is a need for more systematic reconstruction of seasonal climate changes.

8. Lines 52–59: Please add references to Zumaque et al. (2025) and Lapellegerie et al. (2024) (DOI: 10.1016/j.quascirev.2024.109016), which present a chironomid-inferred July temperature reconstruction for the last glacial period from Lake Bergsee.

We have added these references. Please see the highlighted part in the revised text above.

9. Line 57: Please correct the citation year for Zander et al. to 2024 (not 2023).

We have now corrected this. Please see the highlighted part in the revised text above.

10. Line 75: The sentence "Modern pollen data were obtained from version 3 of the SPECIAL Modern Pollen Dataset (SMPDSv3)" requires a reference. Please also clarify how this version differs from the modern pollen dataset by Davis et al. What type of samples does SMPDSv3 include (e.g., surface soils, top-core sediments)? Additionally, please provide details on how climate parameters were derived—were they based on WorldClim or another dataset?

Davis et al is the Eurasian Modern Pollen Database (EMPD), version 2, which has been included in our dataset.

Data Sources

Source	Originally from smpdsv2
Herzschuh et al., 2019	✓
Neotoma	✓
EMPDv2	✓
Bush et al., 2020	✓
SMPDSv1	✓
Australian pollen	✓
EMBSeCBIO	✓
Phelps et al., 2020	✓
CMPD	✓
BIOME6000 Japan	✓
Gaillard et al., 1992	✓
IBERIA	✓
Dugerdil et al., 2021	✓
AMSS	✓
Blyakharchuk	✓
APD	✓
Southern Hemisphere pollen	✓
Harrison et al., 2021	✓
AWI	-
Cao et al.	-
Pangaea	-
EPD	-
Alpine PD	-

We obtained our climate values based on Climatic Research Unit Time-Series version 4.04 (CRU TS4.04; Harris et al., 2020) dataset. We have added the reference and expanded the description of the SMPDSv3 as follows:

Modern pollen data were obtained from version 3 of the SPECIAL Modern Pollen Dataset (SMPDSv3) (Harrison et al., 2025a). This global dataset was constructed by amalgamating and standardising records from public repositories (e.g. Neotoma, Pangaea), existing regional databases (e.g. European Modern Pollen Database, African Pollen Database), individual publications and records provided by the original authors. The records were carefully screened to remove duplicates that were present in more than one source. The modern samples were obtained from multiple types of record, including pollen traps, surface samples, moss polsters and different types of sediment, including cores from lakes and peatbogs, and section through e.g. fluvial or loess deposits. In cases where the record was radiometrically dated, the database preserves all samples younger than 50 yr B.P. However, some samples were undated and are therefore recorded as modern if a collection date was given or assumed modern if not.

The dataset contains 26704 samples from 18202 different locations, and was created after removing taxa that are not climatically diagnostic (e.g. obligate aquatics, carnivorous species, cultivated plants). The dataset provides several levels of taxonomic aggregation; here we use the most aggregated level, where woody species were generally combined at genus level and herbaceous species at sub-family or family level unless they were palynologically distinctive, occupied distinctive ecological niches and were sufficiently geographically widespread. This "amalgamated" dataset contains relative abundance information for 1367 taxa. These samples were aggregated by location (which is longitude, latitude and elevation) in order to remove duplicates. Counts for *Quercus*, *Quercus* (deciduous) and *Quercus* (evergreen) were combined because of inconsistent differentiation of *Quercus* pollen in different regional records. Deciduous and evergreen oaks occupy different areas of climate space, particularly in terms of seasonal moisture; specifically, evergreen oaks are typically found in areas

characterised by winter rainfall such as the Mediterranean. Nevertheless, since there are other plant taxa that are similarly diagnostic of such regimes, the amalgamation of *Quercus* (deciduous) and *Quercus* (evergreen) should not have a major effect on the robustness of our climate reconstructions. We have tested this assumption by making reconstructions based on all taxa except *Quercus* (Supplementary Materials, section 4). Taxa that occurred in less than 10 samples in the training dataset were not used to make reconstructions because it is unlikely that the available samples provided a reasonable estimate of the climate space occupied by these rare taxa (Liu et al., 2020). After the location aggregation and the taxa filter, the dataset contains information on 18202 samples with relative abundance information for 609 taxa (Figure 1a).

We focus on three climate variables: mean temperature of the coldest month (MTCO), mean temperature of the warmest month (MTWA), and a plant-available moisture index (α_{plant}) defined as the estimated ratio of actual to equilibrium evapotranspiration. These three variables reflect ecophysiological controls on plant distribution (Harrison, 2020; Woodward, 1987) that have been shown to independently influence the distribution and abundance of plant species (Boucher-Lalonde et al., 2012; Wang et al., 2013; Wei et al., 2020). α_{plant} is a transformation of the commonly used moisture index MI (defined as the estimated ratio of annual precipitation to annual potential evapotranspiration) that emphasizes differences at the dry end of the climate range, which have a more pronounced effect on vegetation distribution than differences at the wet end (Prentice et al., 2017). Thus, α_{plant} can be better reconstructed from the pollen records than MI.

The climate values at each SMPDSv3 site were obtained using a geographically-weighted regression (GWR) of climatological values of mean monthly temperature, precipitation, and fractional sunshine hours from the Climatic Research Unit Time-Series version 4.04 (CRU TS4.04; Harris et al., 2020) dataset averaged over the period 1961–1990, which corresponds to the interval from which most of the pollen samples were derived. GWR is to correct for elevation differences between the CRU grid cells and the pollen sites. MTCO and MTWA were taken directly from the GWR. MI was calculated for each site using SPLASH v1.0 (Davis et al., 2017) based on daily values of precipitation, temperature and sunshine hours obtained using a mean-conserving interpolation of the monthly values of each. MI was then transformed to α_{plant} using the parametric Fu-Zhang formulation of the Budyko relationship (Supplementary Materials, section 2). The climate space occupied by SMPDSv3 (Figure S1) samples a reasonable range of global climate space and therefore should provide robust reconstructions of climate changes under glacial conditions.

11. Line 150: The correction for the effect of atmospheric CO_2 on plant water-use efficiency (Figure S2), following Prentice et al. (2022), needs to be described in more detail. Also, I would suggest addressing this point in the Discussion, as it has implications for the interpretation of the results. (See also General comment: The effect of CO_2 on the reconstructed parameters (alpha) need to be discussed in more depth.)

We have expanded the description of the CO_2 correction to provide the motivation for applying such a correction and how this was done, and also added some discussions to compare the corrected and uncorrected plant-available moisture. See point 2 in this response.

12. The following sentence requires further development regarding its causes and mechanisms: "These analyses show that there is an anti-phasing between changes in the northern extratropics and the southern extratropics, with warming in the north and cooling in the south. The largest and most consistent warming during D-O events occurs in Eurasia. There is a significant difference in the warming during winter and summer in the northern extratropics, resulting in an overall reduction in seasonality, but no significant difference in the southern extratropics." Please discuss the possible climatic drivers behind these patterns.

The anti-phasing between northern and southern extratropics and the reduction in seasonality in the northern extratropics, are consistent with a number of different proposed mechanisms. The reconstructions of themselves do not address potential causes or mechanisms, but we have expanded the text to indicate the degree to which the patterns shown are consistent with model experiments that address the potential mechanisms underlying these changes. Please see section 4.3 in revised manuscript.

13. The statement "Site-based reconstructions (e.g. Denton et al., 2022; Zander et al., 2024) suggest much larger cooling in..." would benefit from clarification: which specific sites and proxies are referred to here?

The Denton et al. (2022) paper was inadvertently omitted from the reference list and, in any case is inappropriate here because it is a theory paper rather than providing site-based evidence. We have provided specific information on other site-based reconstructions and have also referred to the Zumarque et al (2025), which does provide site-based evidence for the decoupling of summer and winter changes at a regional scale. See point 6 in this response.

14. We have used a global pollen data set for calibration of the pollen–climate relationships...": Recent studies (e.g., Dugerdil et al., 2021, 2025) have emphasized the advantages of using local datasets and region-specific calibrations. It would be helpful to nuance this point and discuss the potential limitations of global-scale calibration in this context.

Most studies have used regional data sets to construct pollen-climate relationships, and some recent studies have advocated the use of local calibrations even when making reconstructions across e.g. the whole of the northern hemisphere (e.g. Herzschuh et al., 2023). The use of region-specific calibrations does in general produce better statistics for the modern relationship, as Dugerdil et al. (2021, 2025) have shown. However, as pointed out by Chevalier et al. (2020), one important issue is that the calibration data set should have a span that reflects the environmental conditions likely to have been experienced in the fossil record. While regional data sets may adequately sample the range of climate experienced during the Holocene, this could be a significant constraint in seeking to reconstruct conditions during the glacial period.

To make this clearer we have modified the text in the methods section to clarify our motivation for using the global data set as follows (section 4.2 in revised manuscript):

We have used a global pollen dataset for calibration of the pollen-climate relationships. In general, reconstructions of glacial climates have used region-specific data sets (e.g. Dugerdil et al., 2021, 2025; Newnham et al., 2017; Wei et al., 2021; Zumaque et al., 2025). Herzschuh et al. (2023) made this explicit in their reconstructions of northern hemisphere climate over the past 30,000 years, by restricting the modern training data to within a 2000 km radius of individual fossil sites. The use of a region-specific raining data set can be justified on the grounds that it produces better statistics for the modern-day relationship between pollen abundance and specific climate variables. Nevertheless, as pointed out by Chevalier et al. (2020), an important issue is that the modern calibration data set has a span that adequately samples the climate space experienced in the past. The use of a global dataset for calibration makes it possible to sample a larger range of climates, and specifically to reconstruct climates that might be very different from the modern range in that region. For example, reconstructions of past European climate (Figure S8) based on region-specific training dataset would yield less extreme winter temperatures than reconstructed using the global training data set. Although the trend and spatial pattern might not be influenced greatly, the amplitude of change might be underestimated.

The use of a global dataset, rather than region-specific training data, relies on the principle of phylogenetic niche conservatism (Harvey and Pagel, 1991; Qian and Ricklefs, 2004; Wang et al., 2025), which states that traits tend to remain constant over time. This also applies to the climate niche (Crisp and Cook, 2012; Jiang et al., 2023; Peterson, 2011; Wiens et al., 2010; Wiens and Graham, 2005) as evidenced by disjunct distributions of taxa across different continents (Yin et al., 2021). Niche conservatism underpins the fact that the modern distribution of specific genera can be predicted using climate-pollen relationships developed from other regions (e.g. Huntley et al., 1989). However, the use of a global dataset can create issues because of inconsistencies in taxonomic resolution between regions. The necessity for treating all species of *Quercus* as a single taxon, despite the fact that evergreen and deciduous species may occupy distinct climate niches in some regions, is a consequence of this. However, we have shown (Supplementary Materials, section 4) that this has little impact on our reconstructions – largely because the climatic distinction that would be conveyed through separating deciduous and evergreen *Quercus* is also registered by the presence of other taxa. Although the use of a global training dataset for climate reconstructions has not been a common practice, it addresses the need to ensure that the modern training data adequately represents past climate conditions and also facilitates making reconstructions for sites from regions with limited modern pollen data.

We have also created a new Figure S8 to replace the old Figure S8, to illustrate the impact of using a local calibration compared to the global calibration dataset, using Europe as an example.

New Figure S8: The distribution of European fossil-reconstructed climates using global (black) vs European (red) modern training dataset.

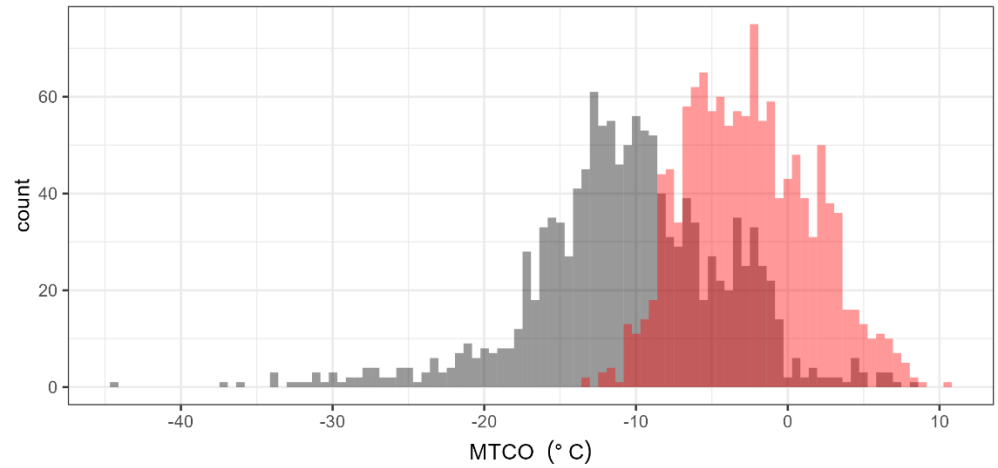

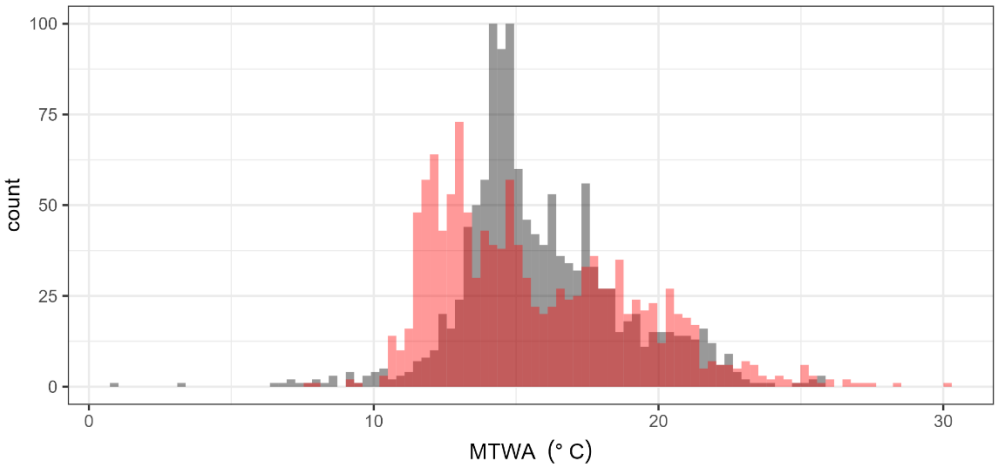

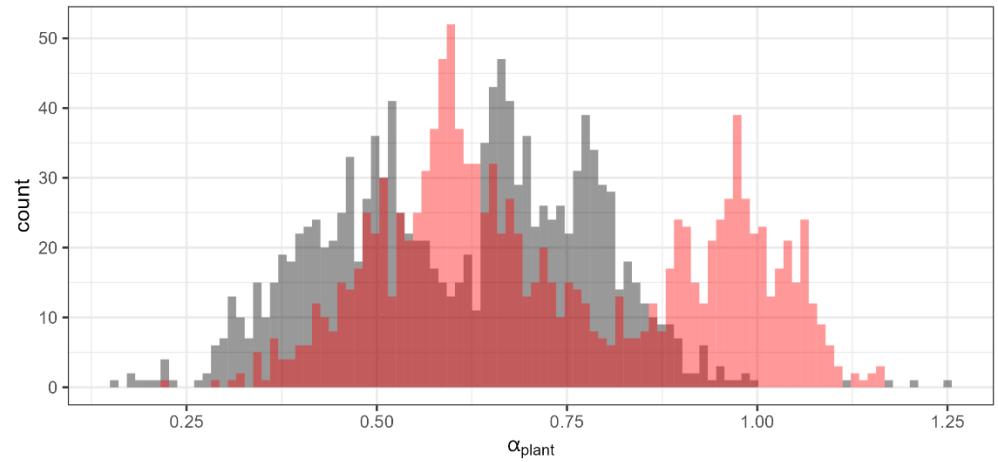

15. I would appreciate the inclusion of a table listing all the pollen taxa used here in your datasets.

We have now included a list of all the pollen taxa used for the reconstructions as a note at the end of supplementary material section 1.